Adaptive Virtual Inertia Calculation for a Virtual Synchronous Generator-Based Building-to-Building Grid

Mhret Berhe Gebremariam
dept. Electrical Engineering
University of Oviedo
Gijon, Spain
gebremariammhret@uniovi.es

Pablo García Fernández
dept. Electrical Engineering
University of Oviedo
Gijon, Spain
garciafpablo@uniovi.es

Ángel Navarro-Rodríguez
dept. Electrical Engineering
University of Oviedo
Gijon, Spain
navarroangel@uniovi.es

Cristian Blanco
dept. Electrical Engineering
University of Oviedo
Gijon, Spain
blancocristian@uniovi.es

***Abstract*—The paper presents an adaptive inertia calculation in a virtual synchronous generator (VSG) based on a building-to-building (B2B) distribution system. Adaptation of the virtual inertia value is done using a disturbance-based approach, following previous literature, which introduces an excitation signal while using voltage, frequency, and power measurements to estimate the inertia. The main benefit of adaptive inertia comes from a reduction in the real power and frequency oscillations, which results in an improvement in the battery system's estimated useful life. The proposed system calculates the virtual inertia of the VSG based on the energy management optimization of the B2B system, based on the photovoltaic (PV), battery state of charge (SoC), and the power exchange between the buildings considering the grid. The system adjusts the virtual inertia with a droop-based control depending on the power exchange between the buildings, and the cost of energy exchange. The proposal is validated by simulation of two buildings in parallel with a grid in MATLAB/SIMULINK.**

***Index Terms*—Microgrid, energy exchange, adaptive control, virtual synchronous generator, power electronics converter.**

I. Introduction

These days, with an increased concern on carbon emission and high energy demand, distributed renewable energy generation systems (REGs) have significantly increased their presence in distributed power systems [1]–[3]. These REGs are integrated into the power system through power electronics converters (PECs), and shall be able to operate either in islanded or grid connected mode. However, the increase in the integration of REGs that has zero or low rotating inertia results in a decreased global system inertia, which potentially can affect the system frequency and stability [4], [5]. The inertia of the system plays a vital role in maintaining the stability of the power system when it is exposed to power imbalance [6]. Taking into consideration the effect of a decrease in inertia, different researches and projects are currently ongoing to provide virtual inertia by using the concept of VSG [1], [7]–[10].

On a VSG-based control system, selecting the values of the virtual inertia and damping factor are the main challenges. In some of the previous researches, the virtual inertia is set to a constant value after making a stability analysis study [11], [12]. Setting a constant inertia value does not consider the change in the PV and battery generation during operation [4]. In [13]–[15], it is proposed to use active power disturbance signals, frequency, and voltage measurement approach to estimate the virtual inertia value by relying on the rate of change of frequency. In these methods, the power loss must be known accurately, and it is difficult to estimate the parameters after an event has occurred when multiple changes in the generation occur. The accuracy of calculating the rate of change of frequency (RoCoF) also affects the inertia estimation accuracy. Other online inertia estimation methods are presented in [16]–[18]. However, most of them are dependent on recorded historical data. Recent research studies focus on forecasting virtual inertia using intelligent programming systems such as fuzzy logic, and artificial neural network (ANN) [19]–[21].

The main objective of this paper is to propose an adaptive virtual inertia calculation based on B2B power exchange. The system considers a VSG-based B2B energy exchange microgrid model presented in [22]. The B2B system considers buildings with PV generation, ESS, in-building load. It is connected to other buildings and the grid through a VSG-controlled inverter to allow power exchange. The inertia contribution of the buildings in the B2B system is analyzed depending on the building generation, ESS, and the power exchange between the buildings and the grid together with the price of power exchange. The adaptive inertia calculation is done with a droop-based control using the price offered by the buildings to exchange power, and the minimum and maximum inertia the buildings can contribute. The inertia contribution takes into consideration the generation and the depth of discharge of the ESS to limit the maximum inertia the building can contribute to the microgrid system. Two grid-tied parallel buildings are considered to validate the operation of the proposed adaptive inertia calculation in a B2B system.

The present work has been partially supported the European Union's H2020 Research and Innovation programme under Grant Agreement No 864459 (UE-19-TALENT-864459) and by the Spanish Ministry of Innovation and Science uder Grant MCI-20-PID2019-111051RB-I00 funded by MCIN/AEI/10.13039/501100011033.

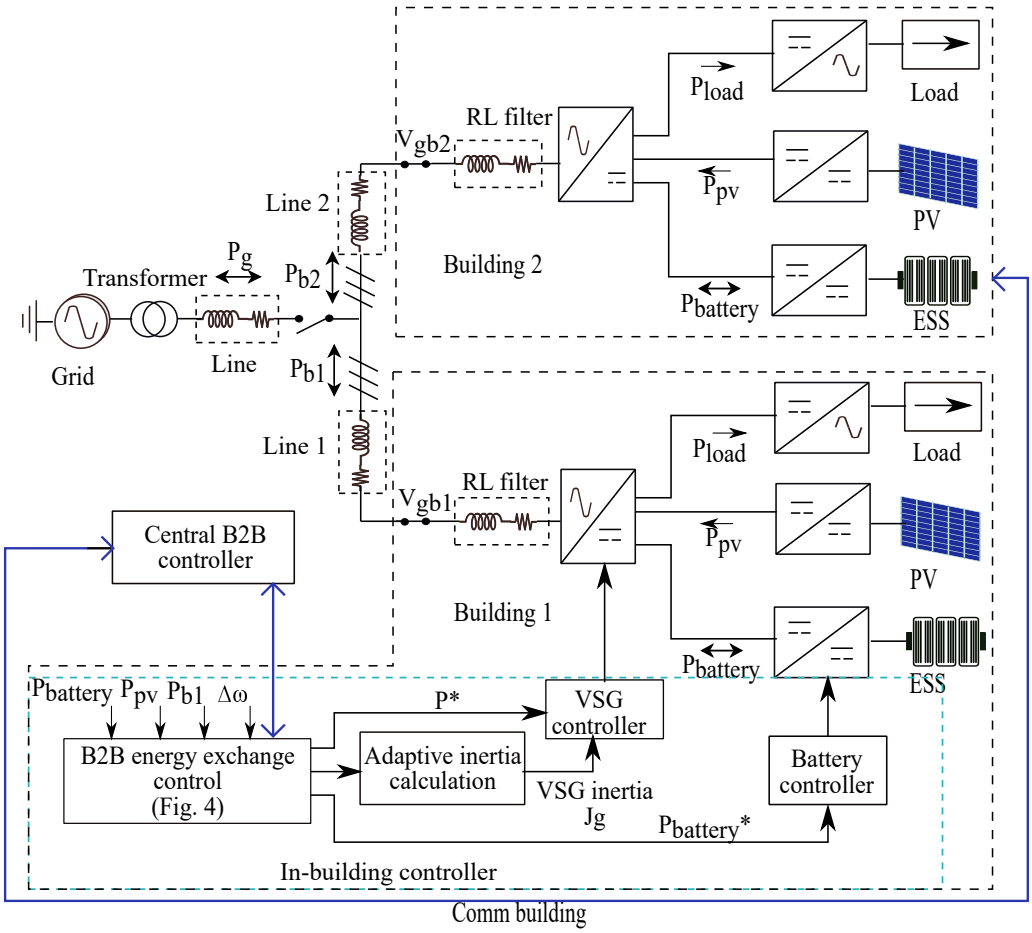

Fig. 1. Schematics of the proposed system.

II. Control System Design

The proposed system uses a B2B microgrid system which was presented in [22]. It considers PV generation, ESS and loads in the building internal grid, and a VSG-based DC/AC interlinking inverter, as shown in Fig.1. The system has an in-building central controller which receives the voltage and frequency references from the central B2B controller.

The VSG control system contains the swing equation (1) that mimics the behavior of a synchronous generator, where J is the virtual inertia, D the mechanical damping, and T_e and T_m are electrical and mechanical torque.

$$J\frac{d\omega_r}{dt} = (T_m - T_e) - D_p\Delta\omega \tag{1}$$

The swing equation in the VSG control receives the inertia value from the adaptive inertia calculation which is proposed in this paper as shown in Fig. 2. The governor and AVR models are considered as a $\omega - P$ and $V - Q$ droop controllers. The voltage reference output E from the AVR model is fed to the impedance model of the VSG system to calculate the current references for the current controller as shown in Fig. 2.

The ESS and PV generation are connected to the system through DC/DC converters. The reference power of the ESS and the grid is provided from the B2B power exchange controller as shown in Fig. 1. The detail operation of the VSG controller with a droop based dc-link voltage control is presented at [22]. The proposed system is simulated in MATLAB/SIMULINK using two buildings in parallel with a grid. The operation of the proposed system is validated with variations in the power generation from PV, and load demand. A comparison of the proposed system and constant inertia $\Delta\omega$ response is presented. Power exchange between the buildings, and the buildings and the grid are introduced to observe the response of the system to maintain the system stability.

A. Building to Building Energy Exchange

The proposed system considers a number of buildings with PV generation, ESS, and the in-building load connected to the grid with a VSG controlled interlinking inverter. The energy exchange between the buildings is done based on the generation, load demand, SoC of ESS, cost of charging and discharging the ESS, the price offered by other buildings $Price_{offered}$ to buy P_{buyOB} amount of power, and the price request $Price_{request}$ to sell the extra $P_{availableOB}$ amount of power they have. The battery degradation cost of charging and

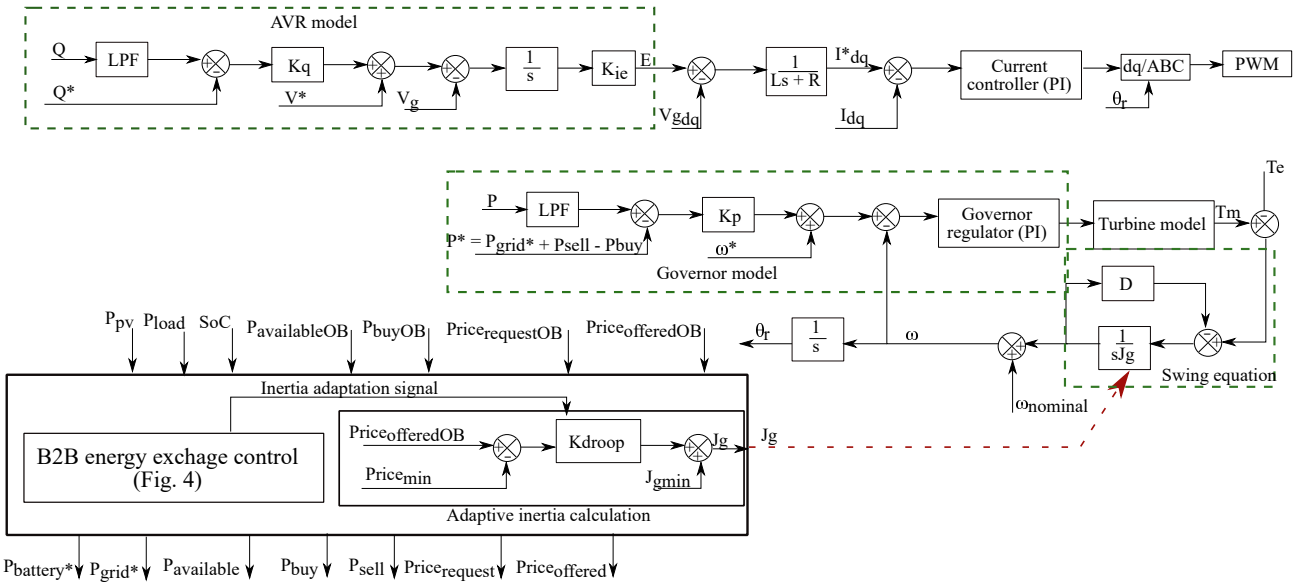

Fig. 2. Proposed controller architecture.

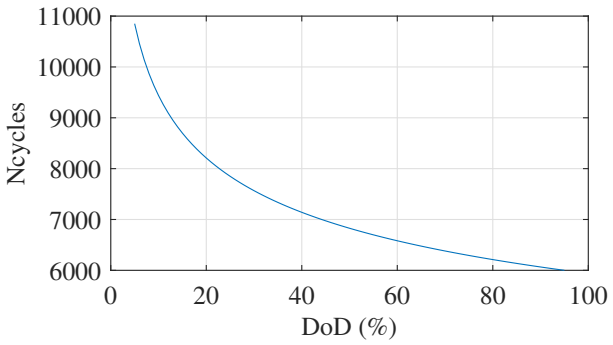

Fig. 3. Number of cycle of a battery versus the depth of discharge (DoD).

discharging the battery is calculated using [23]:

$$C_E = C_{capital}/N_{cycles} \tag{2}$$

Where $C_{capital}$ is the capital cost of the battery, and N_{cycles} is number of cycles depending on the depth of discharge (DoD) from the experimental result of battery as shown in Fig. 3. The power exchange between the buildings and the grid, with the optimization of battery charging and discharging is done using the method shown in Fig. 4. Each building has access to the data of the available power for sell, power demand to buy, the price offered, price request, and the type of generation of other buildings through the central controller. The price offered by the grid to supply power from the buildings to the grid, and the PV generation cost in the day time is considered to be 0. The system decides the adaptation of the virtual inertia depending on the power exchange between the buildings, and the grid as shown in Fig. 4. When the PV generation is greater than the power demand, the system decides whether to charge its battery or sell power to other buildings or grid based on the SoC of the battery, the cost of charging, price offered by other buildings or grid. If the price offered by other building is high, the building sells power to other buildings and adapts its inertia depending on the price they are offering. Otherwise, if the battery is full, it exchanges power with the grid and adjusts its inertia depending on the price offered by the grid as shown in Fig. 4. Similarly, when load demand is greater than the PV generation, the system decides whether to discharge its battery or buy power from other buildings or the grid as shown in Fig. 4. When the other buildings have available power and the price is less than the cost of discharging the battery, the building buys power from other buildings depending on the price request and the greenness of the energy, and adapts its inertia. When the battery is not able to supply power, the system compares the price request by other buildings and the grid, decides to buy the cheapest and green energy, and adapts its inertia as shown in Fig. 4.

B. Adaptive Inertia controller

Inertia in a power system refers to the capability to maintain the system stability when a disturbance is introduced. Power systems with large synchronous generators are able to maintain the frequency and voltage to a rated value. To maintain system stability when integrating REGs, it is desired to use a control system that can incorporate inertia emulation. The swing equation given in (1) can be written as (3) [19]:

$$J\omega_r \frac{d\omega_r}{dt} = (P_m - P_e) - D\Delta\omega \tag{3}$$

Where P_m is the mechanical power, P_e is the electrical power, and $D = \frac{\Delta P_{max}}{\omega_0 \Delta\omega_{max}}$. For the proposed B2B system the ΔP is the sum of PV, ESS and grid power changes. For a power system with different generations and inertia units, the overall inertia is defined as (4).

$$H_s = \frac{\sum_{i=1}^{N} H_i S_{B,i}}{S_B} \tag{4}$$

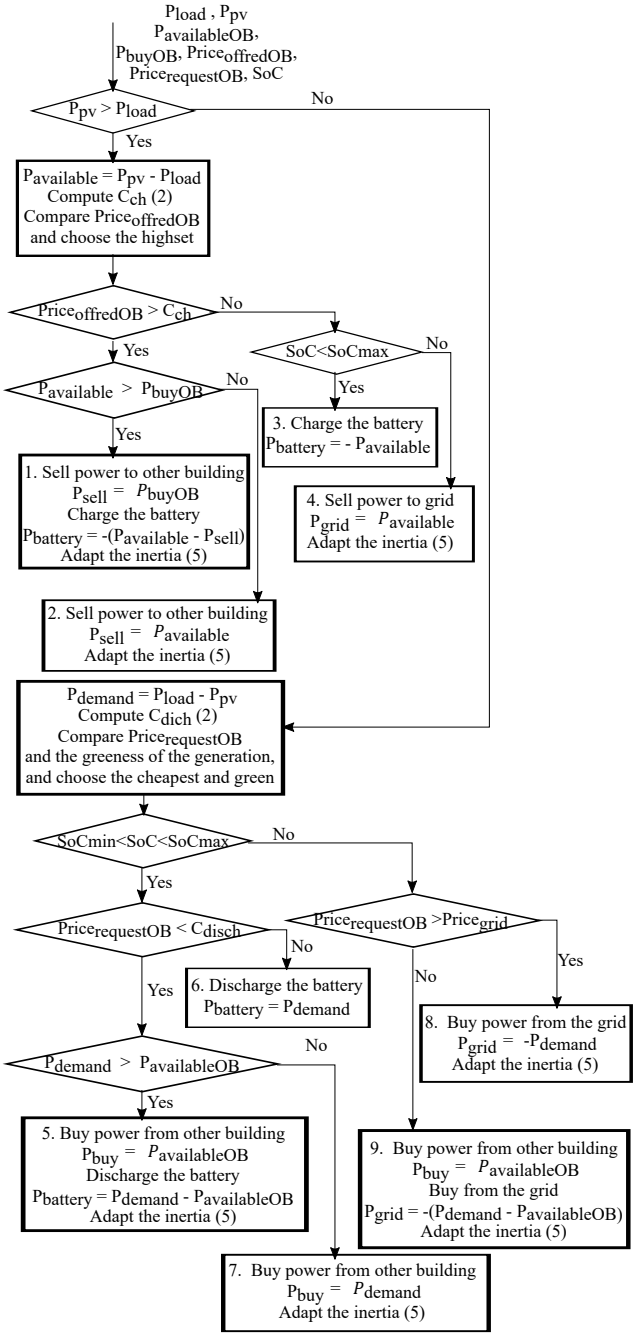

Fig. 4. B2B power exchange control scheme.

Where H_s is the virtual inertia constant in seconds given by $\frac{1}{2}J\frac{\omega_b^2}{S_b}$, H_i and S_{Bi} are the inertia constant and power rating of individual generators in the system, and S_B is the power rating of the power system. For the VSG system, the sum of PV and ESS is considered as generation to calculate the inertia contribution of the building to the power system. Considering (4), in a B2B system inertia of each building contributes to the inertia of the power system. Hence, adaptation of the inertia of each building is done based on the power exchange between the buildings and the price offered by other buildings in a droop based calculation as shown in (5).

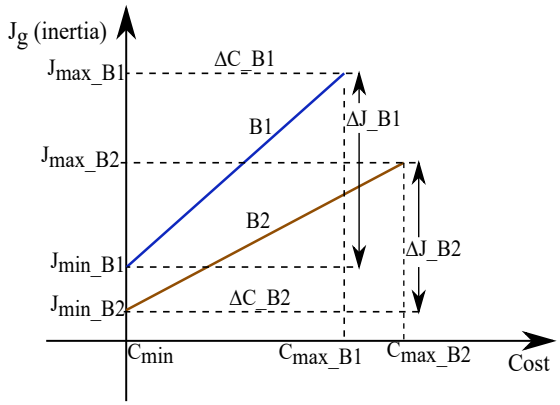

Fig. 5. Proposed droop based cost-inertia characteristics

TABLE I
SYSTEM PARAMETERS

Parameter	Value
Dc bus voltage	750 V
Ac side voltage	230 V
Rated power	100 kVA
Nominal frequency f_0	50 Hz
Reference virtual inertia J_0/J_{gmin}	0.426 kgm^2
RL filter inductance/resistance	0.5 mH/ 0.01 Ω
Droop coefficients K_p/K_q	$3.49x10^{-5}$/ $4.57x10^{-4}$
Inertia droop coefficient K_{droop}	7.74
Battery capital cost $C_{Capital}$	400 euro/kWh

$$J_g = J_{gmin} + K_{droop}\Delta C \tag{5}$$

$$K_{droop} = \frac{J_{gmax} - J_{gmin}}{C_{max} - C_{min}} \tag{6}$$

Where C_{max} and C_{min} are the maximum and minimum $Price_{offered}$ by other buildings to buy energy, and K_{droop} is the inertia droop coefficient. During power exchange with other buildings and the grid, the building provides an inertia support depending on the price offered by other buildings as shown in (5) and Fig 5. As the cost of power exchange depends on the amount of power exchange between the buildings and the grid, the inertia adaptation is dependent on the amount of power exchange and the frequency variation it can introduce. The higher the price offered by other buildings, the higher the inertia support it will provide without exceeding the maximum inertia. Changes in the P_{pv}, P_{load} for both the buildings 1 and 2 are introduced to verify the operation of the proposed system.

III. SIMULATION RESULTS

In order to validate the operation of the proposed system, a simulation for the configuration shown in Fig. 1 using the proposed adaptive inertia control is conducted in MATLAB/SIMULINK. Taking into account the power rating of the proposed power system which is 100 kVA, the reference virtual inertia constant H is set to 0.21 s (3).
For building 1, PV generation and load demand power changes are introduced at:

- 2 s PV generation change from 0 to 40 kW.
- 4 s load demand change from 0 to 20 kW.
- 7 s load demand change from 20 to 15 kW.
- 8 s PV generation change from 40 to 60 kW.
- 9 s load demand change from 15 to 20 kW.
- 12 s PV generation from 60 to 40 kW.
- 13 s load demand change from 20 to 70 kW as shown in Fig. 6a.

Similarly for building 2, PV generation and load demand power changes are introduced at:

- 4 s PV generation change from 0 to 20 kW.
- 5 s load demand change from 0 to 40 kW.
- 7 s load demand change from 40 to 20 kW.
- 8 s PV generation change from 20 to 30 kW.
- 9 s load demand change from 20 to 40 kW.
- 11 s load demand change from 40 to 30 kW.
- 14 s PV generation change from 30 to 20 kW.
- 17 s load demand change from 30 to 60 kW as shown in Fig. 6b.

The B2B energy exchange between the buildings and the grid is made based on the control presented in Fig. 4.

- At 2 s - 4 s, building 1 has $P_{pv} > P_{load}$, and there is no request by other buildings to buy power, so it is charging its battery.
- At 4 s - 5 s, both building 1 and 2 has $P_{pv} > P_{load}$, and they are charging their battery as shown in Fig. 6e as there are no other buildings requesting to buy power from the buildings and the price to supply power to the grid is considered 0.
- At 5 s - 7 s, building 1 has $P_{pv} > P_{load}$, and building $P_{pv} < P_{load}$. At this time building 1 stops charging its battery and starts selling 20 kW power to building 2 as shown in Fig. 6c and a.
- At 7 s - 8 s, building 1 has $P_{pv} > P_{load}$, and building $P_{pv} = P_{load}$. At this time, building 2 has enough power to supply its load and stops buying power from building 1, and building 1 starts charging its battery with the extra power as shown in Fig. 6a and b.
- At 8 s - 9 s, both buildings 1 and 2 has $P_{pv} > P_{load}$, and both charges their battery.
- At 9 s - 11 s, building 1 has $P_{pv} > P_{load}$, and building $P_{pv} < P_{load}$. At this time building 1 is selling 10 kW power to building 2, and at the same time charging its battery with the extra power as shown in Fig. 6c and a.
- At 11 s - 13 s, building 1 has $P_{pv} > P_{load}$, and building $P_{pv} = P_{load}$. At this time building 2 is supplying its load and doesn't have extra power to sell, but building 1 has extra generation and charges its battery as shown in Fig. 6c, a and b as the price offer by the grid to supply power from the building to the grid is considered to be 0.
- At 13 s - 14 s, building 1 has $P_{pv} < P_{load}$. As it was charging its battery before and cost of discharging the battery is less than cost of importing power from the grid, it starts discharging its battery to supply its load demand.

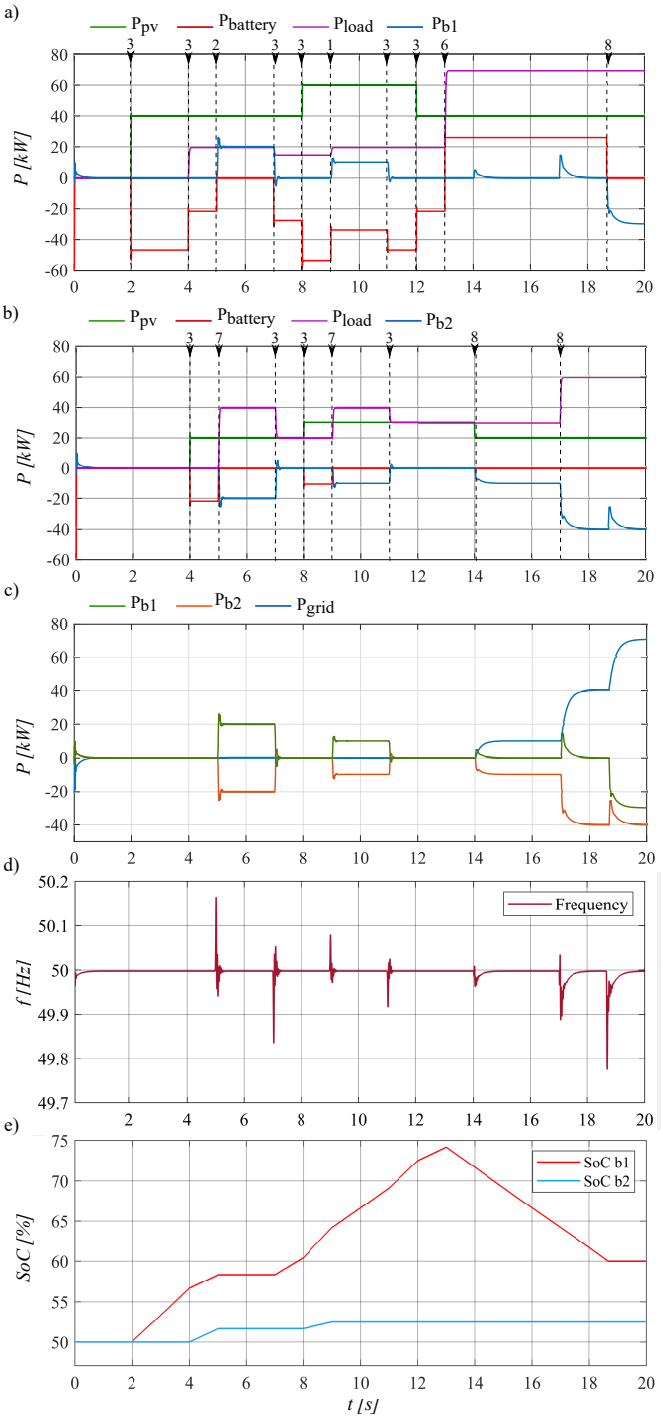

Fig. 6. Power measurements of the B2B simulation with variation in p_{pv} and p_{load} of the buildings with condition labeling based on Fig. 4, a) Power measurement results of building 1, b) Power measurement results of building 2, c) B2B and grid power measurement results, d) Building level frequency of V_{gb1}, e) Battery SoC of building 1 and 2.

- At 14 s - 19 s, building 2 has $P_{pv} < P_{load}$, and there is no available power for sell from building 1, so building 2 starts buying power from the grid, and building 1 continues to discharge its battery as shown in Fig. 6a, b and c.
- At 19 s - 20 s, for both buildings 1 and 2 the cost of

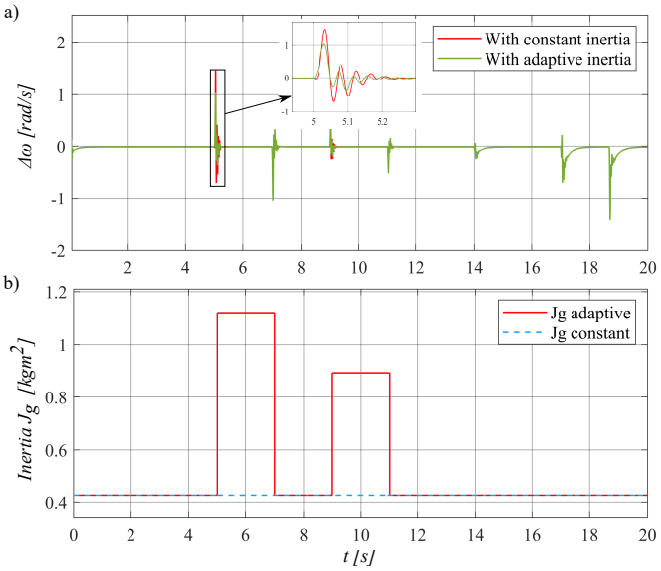

Fig. 7. Simulation results comparison of adaptive and constant inertia control (Power exchange from building 1 to building 2 at 5 s - 7 s and 9 s - 11 s), a) Power measurement results of building $\Delta\omega$ with constant and adaptive inertia control, b) Virtual inertia J_g with constant and adaptive inertia control.

discharging the battery is higher than cost of importing power from the grid, and there is no available power from other buildings, so both the buildings buy power from the grid as shown in Fig. 6a, b and c.

With the load and generation changes shown in 6a and b, the system is able to maintain the frequency in the building level measured at V_g (Fig. 1) within the required limits of $\pm 1\% f_0$ as shown in Fig. 6d. Fig. 7b shows the virtual inertia J_g with a constant inertia, and adaptive inertia control. As shown in Fig. 7b, the adaptive control changes its inertia when the building is exchanging power with the other buildings at 5 s - 7 s and 9 s - 11 s based on the $Price_{offeredOB}$ by the other building to buy power. Even though the buildings are exchanging power with the grid at 14 s - 20 s, the system inertia is kept minimum as the price offer by the grid is considered 0. Fig. 7a shows $\Delta\omega$ with a constant inertia, and adaptive inertia control. As it can be seen the adaptive inertia calculation based control is able to minimize $\Delta\omega$ compare to the constant inertia based control.

IV. Conclusion

This paper has presented an adaptive virtual inertia control for a VSG based on the B2B grid system. The proposed system allows power exchange between buildings and grid, and improves the frequency transient of the power system at the building level by allowing adaptive calculation of the virtual inertia contribution by the VSG based control, depending on the power exchange between the buildings and the price offered by other buildings to buy power. The shown simulation results corroborate this feature. The proposed system is validated using MATLAB/SIMULINK simulation for a two building system.

References

[1] J. Liu, Y. Miura, and T. Ise, "Comparison of dynamic characteristics between virtual synchronous generator and droop control in inverter-based distributed generators," *IEEE Transactions on Power Electronics*, vol. 31, no. 5, pp. 3600–3611, 2015.

[2] K.-H. Tan, F.-J. Lin, C.-M. Shih, and C.-N. Kuo, "Intelligent control of microgrid with virtual inertia using recurrent probabilistic wavelet fuzzy neural network," *IEEE Transactions on Power Electronics*, vol. 35, no. 7, pp. 7451–7464, 2019.

[3] K.-H. Tan and T.-Y. Tseng, "Seamless switching and grid reconnection of microgrid using petri recurrent wavelet fuzzy neural network," *IEEE Transactions on Power Electronics*, 2021.

[4] E. Heylen, F. Teng, and G. Strbac, "Challenges and opportunities of inertia estimation and forecasting in low-inertia power systems," *Renewable and Sustainable Energy Reviews*, vol. 147, p. 111176, 2021.

[5] F. Gonzalez-Longatt, J. M. Roldan-Fernandez, H. R. Chamorro, S. Arnaltes, and J. L. Rodriguez-Amenedo, "Investigation of inertia response and rate of change of frequency in low rotational inertial scenario of synchronous dominated system," *Electronics*, vol. 10, no. 18, p. 2288, 2021.

[6] P. Makolo, R. Zamora, and T.-T. Lie, "Online inertia estimation for power systems with high penetration of res using recursive parameters estimation," *IET Renewable Power Generation*, vol. 15, no. 12, pp. 2571–2585, 2021.

[7] Q.-C. Zhong and G. Weiss, "Synchronverters: Inverters that mimic synchronous generators," *IEEE Transactions on industrial electronics*, vol. 58, no. 4, pp. 1259–1267, 2010.

[8] U. Tamrakar, D. Shrestha, M. Maharjan, B. P. Bhattarai, T. M. Hansen, and R. Tonkoski, "Virtual inertia: Current trends and future directions," *Applied Sciences*, vol. 7, no. 7, p. 654, 2017.

[9] A. Navarro-Rodríguez, P. García, R. Georgious, J. García, and S. Saeed, "Observer-based transient frequency drift compensation in ac microgrids," *IEEE Transactions on Smart Grid*, vol. 10, no. 2, pp. 2015–2025, 2019.

[10] A. Navarro-Rodríguez, P. García, C. Blanco, R. Georgious, and J. García, "Cooperative control in a hybrid dc/ac microgrid based on hybrid dc/ac virtual generators," in *2018 IEEE Energy Conversion Congress and Exposition (ECCE)*, 2018, pp. 1156–1163.

[11] V. Mallemaci, F. Mandrile, S. Rubino, A. Mazza, E. Carpaneto, and R. Bojoi, "A comprehensive comparison of virtual synchronous generators with focus on virtual inertia and frequency regulation," *Electric Power Systems Research*, vol. 201, p. 107516, 2021.

[12] F. S. Rahman, T. Kerdphol, M. Watanabe, and Y. Mitani, "Optimization of virtual inertia considering system frequency protection scheme," *Electric Power Systems Research*, vol. 170, pp. 294–302, 2019.

[13] D. Zografos, M. Ghandhari, and R. Eriksson, "Power system inertia estimation: Utilization of frequency and voltage response after a disturbance," *Electric Power Systems Research*, vol. 161, pp. 52–60, 2018.

[14] C. Phurailatpam, Z. H. Rather, B. Bahrani, and S. Doolla, "Measurement-based estimation of inertia in ac microgrids," *IEEE Transactions on Sustainable Energy*, vol. 11, no. 3, pp. 1975–1984, 2019.

[15] B. Wang, H. Sun, W. Li, C. Yang, W. Wei, B. Zhao, and S. Xu, "Power system inertia estimation method based on maximum frequency deviation," *IET Renewable Power Generation*, vol. 16, no. 3, pp. 622–633, 2022.

[16] K. Tuttelberg, J. Kilter, D. Wilson, and K. Uhlen, "Estimation of power system inertia from ambient wide area measurements," *IEEE Transactions on Power Systems*, vol. 33, no. 6, pp. 7249–7257, 2018.

[17] J. D. Lara-Jimenez, J. M. Ramırez, and F. Mancilla-David, "Allocation of pmus for power system-wide inertial frequency response estimation," *IET Generation, Transmission & Distribution*, vol. 11, no. 11, pp. 2902–2911, 2017.

[18] X. Cao, B. Stephen, I. F. Abdulhadi, C. D. Booth, and G. M. Burt, "Switching markov gaussian models for dynamic power system inertia estimation," *IEEE Transactions on Power Systems*, vol. 31, no. 5, pp. 3394–3403, 2015.

[19] K.-H. Tan, F.-J. Lin, T.-Y. Tseng, M.-Y. Li, and Y.-D. Lee, "Virtual synchronous generator using an intelligent controller for virtual inertia estimation," *Electronics*, vol. 11, no. 1, p. 86, 2022.

[20] W. Xing, H. Wang, L. Lu, X. Han, K. Sun, and M. Ouyang, "An adaptive virtual inertia control strategy for distributed battery energy storage system in microgrids," *Energy*, p. 121155, 2021.

[21] T. Kerdphol, M. Watanabe, K. Hongesombut, and Y. Mitani, "Self-adaptive virtual inertia control-based fuzzy logic to improve frequency stability of microgrid with high renewable penetration," *IEEE Access*, vol. 7, pp. 76 071–76 083, 2019.

[22] M. B. Gebremariam, P. G. Fernandez, C. B. Charro, and A. N. Rodriguez, "Enhanced dc-link voltage control in a virtual synchronous generator-based building-to-building grid considering islanded mode operation," in *2021 IEEE Energy Conversion Congress and Exposition (ECCE)*. IEEE, 2021, pp. 912–918.

[23] J.-O. Lee and Y.-S. Kim, "Novel battery degradation cost formulation for optimal scheduling of battery energy storage systems," *International Journal of Electrical Power & Energy Systems*, vol. 137, p. 107795, 2022.